Electronic Supplementary Material (ESI) for New Journal of Chemistry.

Electronic Supplementary Information

Efficient Cascade Reactions for Luminescent Pyrylium Biolabels Catalysed by Light Rare-Earth Elements

Guangming Wang[a], Xun Li[a], Xuepu Wang[a], and Kaka Zhang*[a]

a G. Wang, X. Li, Dr. X. Wang, Prof. Dr. K. Zhang
Key Laboratory of Synthetic and Self-Assembly Chemistry for Organic Functional Molecules, Shanghai Institute of Organic Chemistry, University of Chinese Academy of Sciences, Chinese Academy of Sciences
345 Lingling Road, Shanghai 200032, People's Republic of China
Email: zhangkaka@sioc.ac.cn

Table of Contents

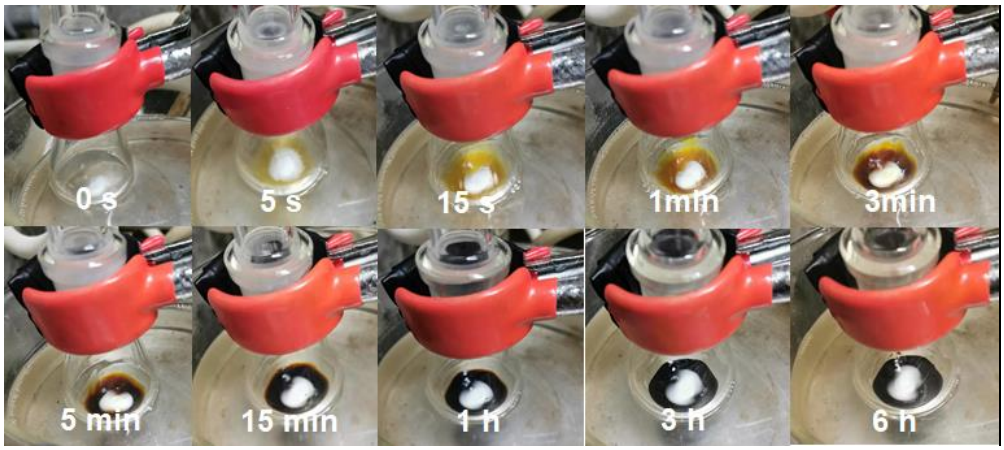

Fig. S1 Color change of the reaction mixture of anisole, acetic anhydride and europium(III) triflate.

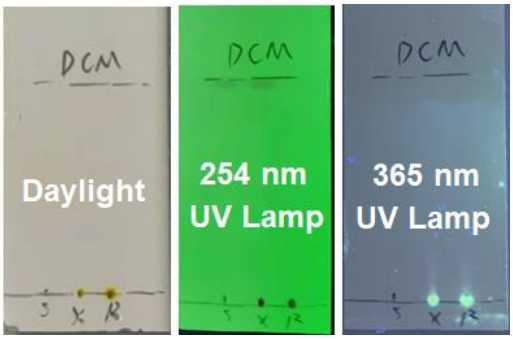

Fig. S2 Thin-layer chromatography of the reaction mixture of anisole, acetic anhydride and europium(III) triflate under day light, 254 nm UV lamp and 365 nm UV lamp. In the TLC plate, S, X, and R represent anisole, anisole and reaction mixture, and reaction mixture, respectively.

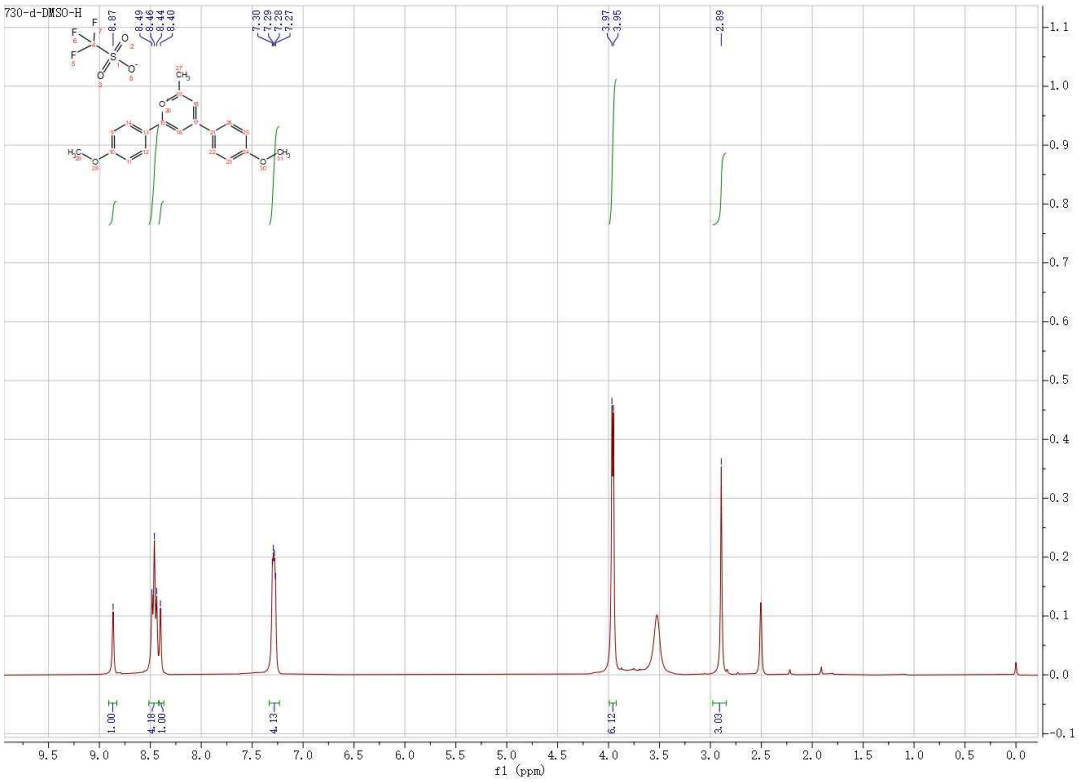

Fig. S3 ^{1}H NMR spectrum of 730 (400 MHz, DMSO-d_6, 298 K).

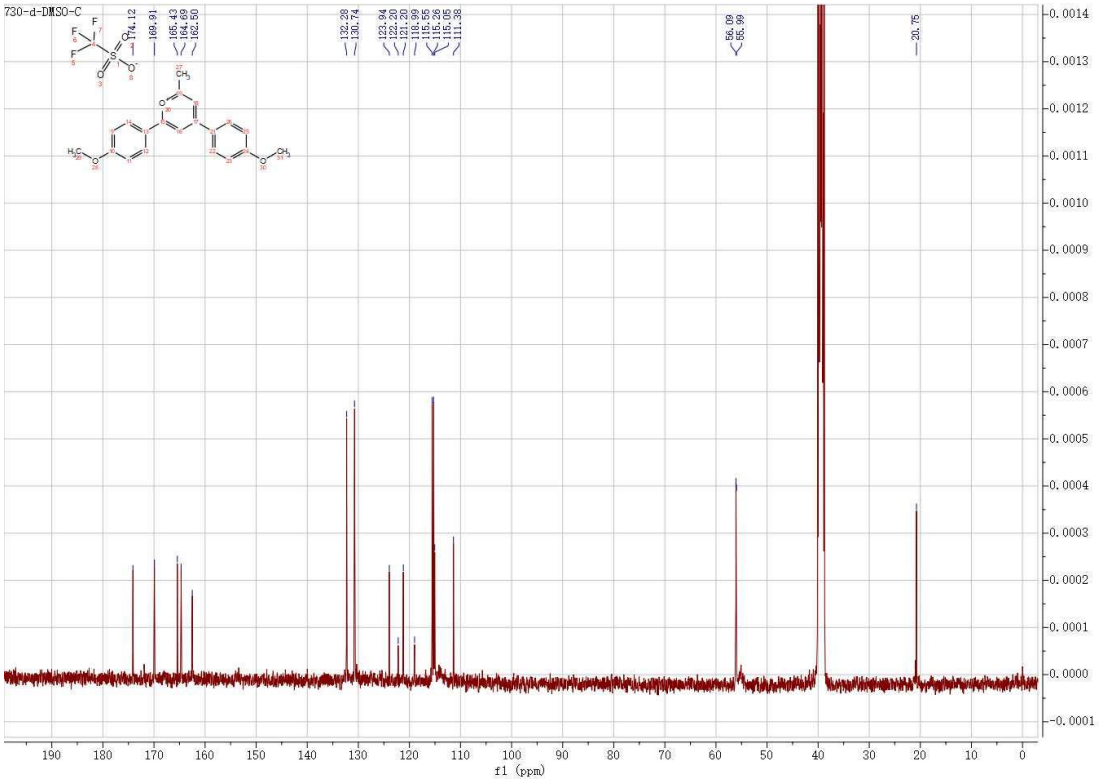

Fig. S4 ^{13}C{^{1}H} NMR spectrum of 730 (100 MHz, DMSO-d_6, 298 K).

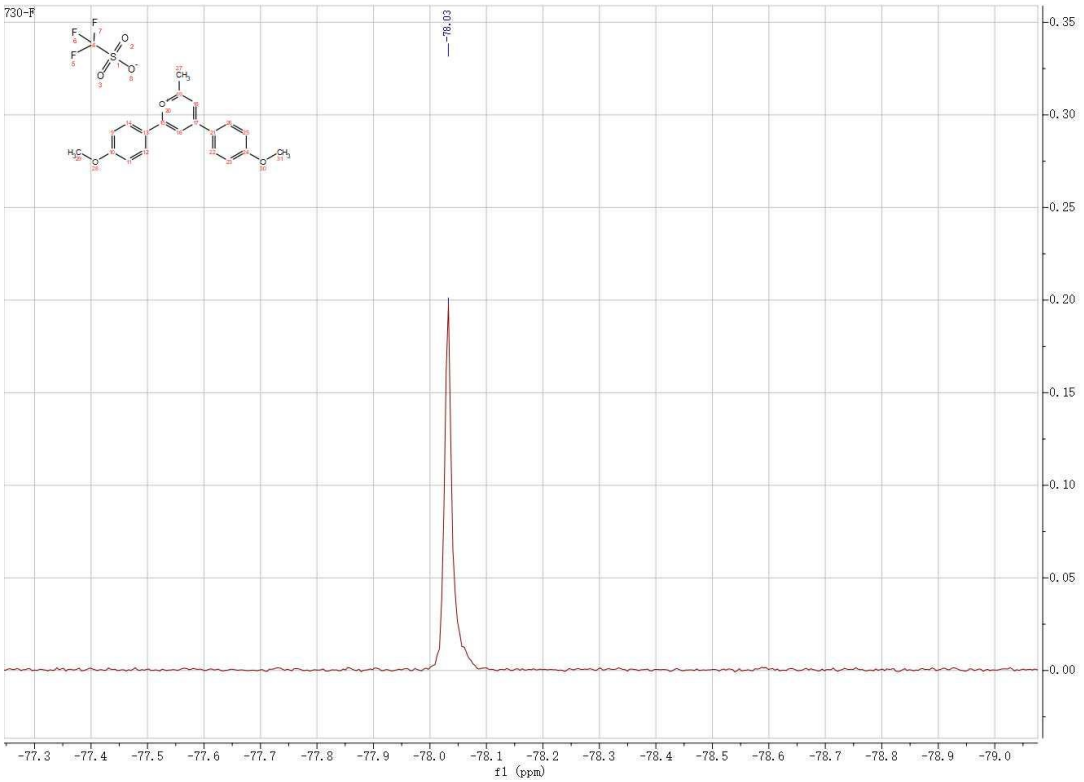

Fig. S5 ^{19}F NMR spectrum of 730 (376 MHz, DMSO-d_6, 298 K).

National Center for Organic Mass Spectrometry in Shanghai
Shanghai Institute of Organic Chemistry
Chinese Academic of Sciences
High Resolution ESI-MS REPORT

Instrument: Thermo Scientific Q Exactive HF Orbitrap-FTMS

Card Serial Number: E202070

Sample Serial Number: Wgm-730

Operator: Songw Date: 2020/10/26

Operation Mode: ESI Positive Ion Mode

Elemental composition search on mass 307.13

m/z= 302.13-312.13

m/z	Theo. Mass	Delta (ppm)	RDB equiv.	Composition
307.1328	307.1329	-0.10	11.5	$C_{20}H_{19}O_3$
	307.1315	4.27	12.0	$C_{18}H_{17}O_2N_3$

Fig. S6 HRMS-ESI report of 730.

National Center for Organic Mass Spectrometry in Shanghai
Shanghai Institute of Organic Chemistry
Chinese Academic of Sciences
High Resolution ESI-MS REPORT

Instrument: Thermo Scientific Q Exactive HF Orbitrap-FTMS

Card Serial Number: E211048

Sample Serial Number: 345730

Operator: Songw Date: 2021/04/02

Operation Mode: ESI Positive Ion Mode

Elemental composition search on mass 427.1749

m/z= 422.1749-432.1749

m/z	Theo. Mass	Delta (ppm)	RDB equiv.	Composition
427.1749	427.1751	-0.61	11.5	$C_{24}H_{27}O_7$

Fig. S7 HRMS-ESI report of 345.

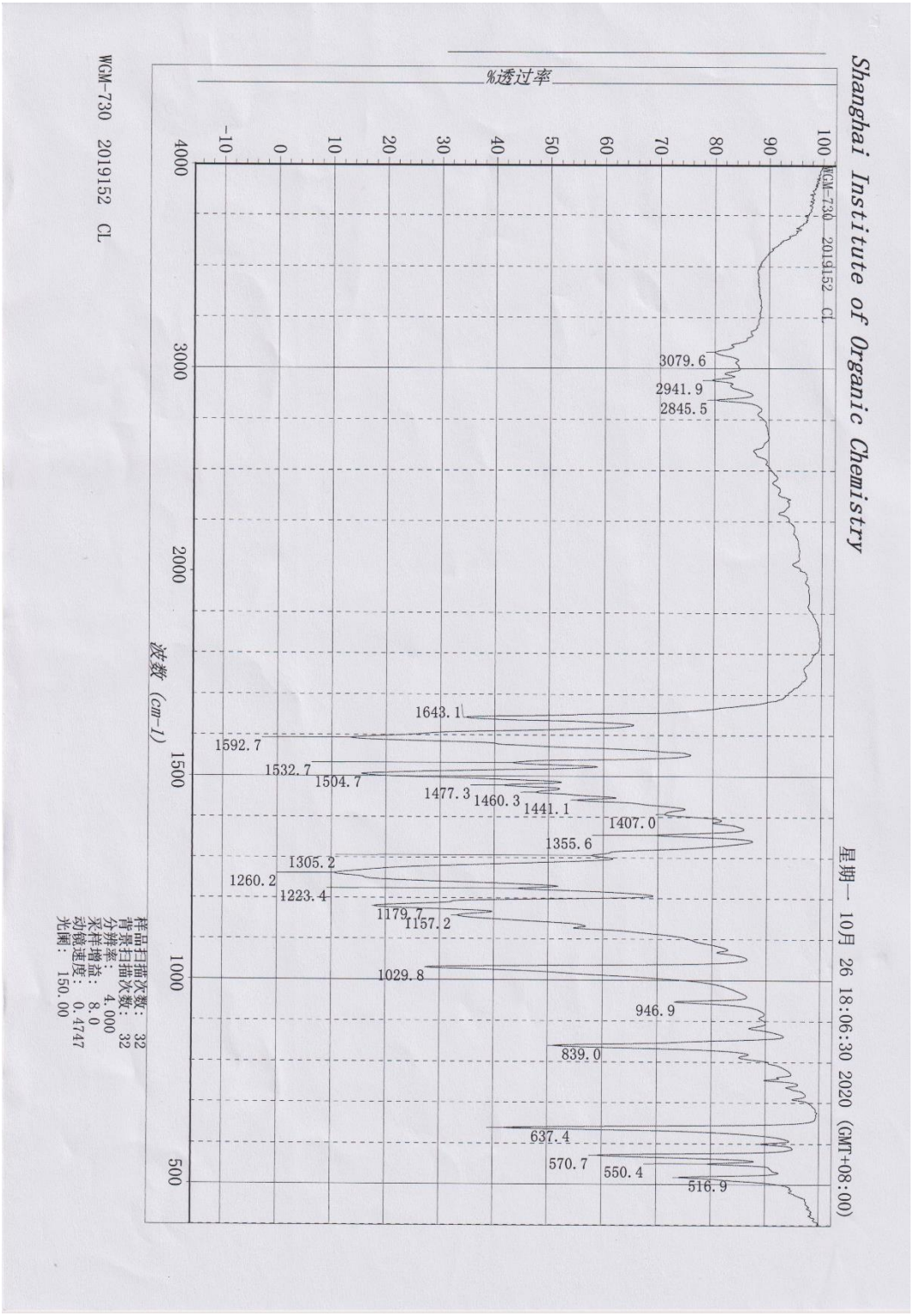

Fig. S8 FT-IR spectrum of 730.

Fig. S9 Photographs of the reaction mixture in control experiments: (left) the reaction mixture of anisole and acetic anhydride; (right) the reaction mixture of anisole and europium(III) triflate.

Fig. S10 Photographs of thin-layer chromatography of the reaction mixture of anisole, acetic anhydride and europium(III) triflate under 254 nm UV lamp. In the TLC plate, S, X, and R represent 4-methoxyacetophenone, 4-methoxyacetophenone and reaction mixture, and reaction mixture, respectively.

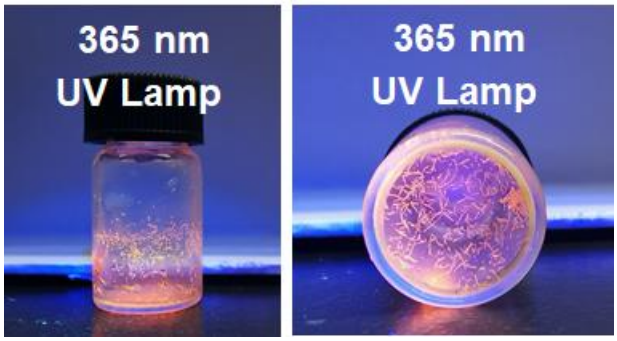

Fig. S11 Photographs of 730 purified by recrystallization in acetonitrile/deionized water.

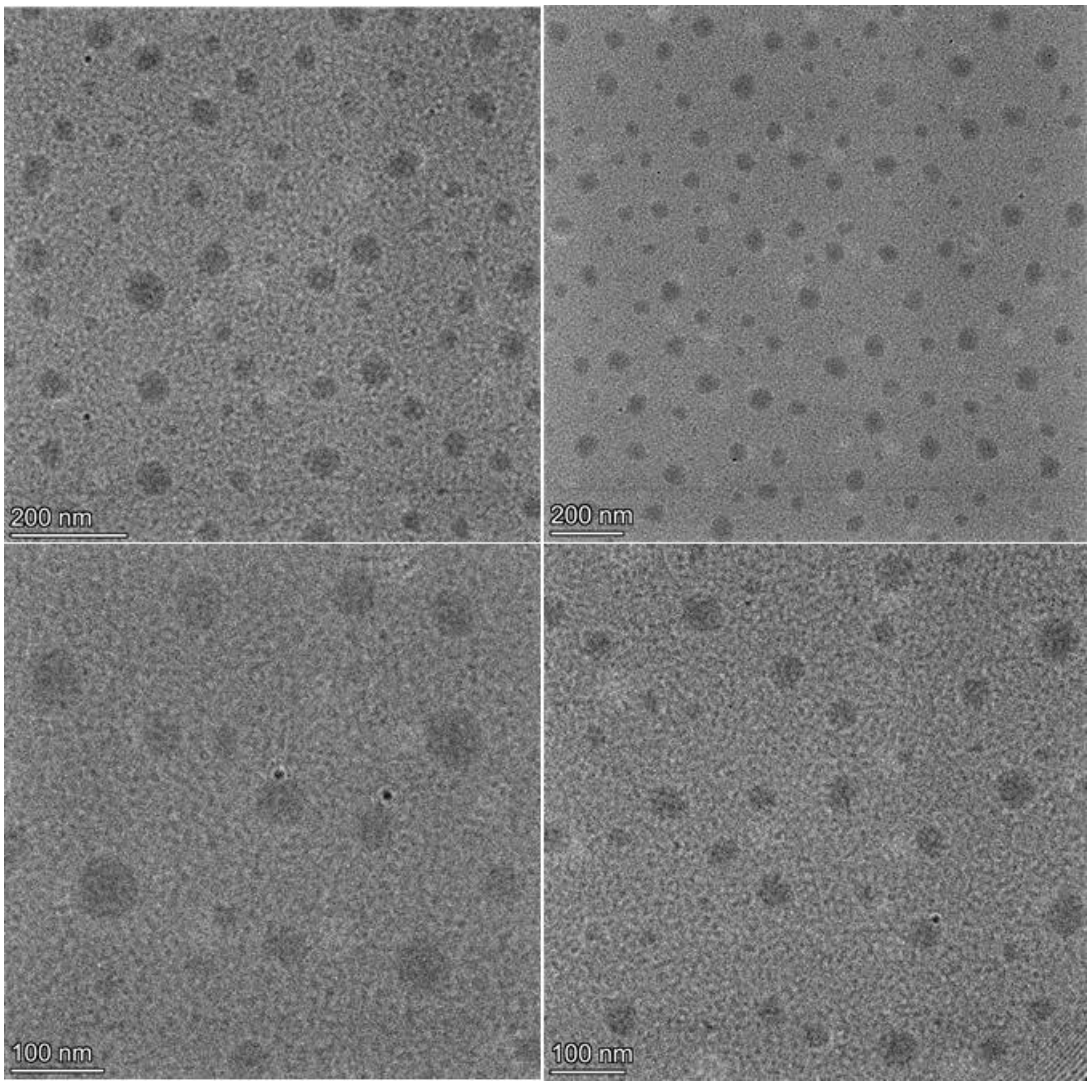

Fig. S12 TEM images of 730NPs. The black dots in the TEM images have smaller sizes (approximately 10 nm) than 730NPs but show a higher electron contrast than 730NPs, which can rule out the possibility that the black dots are formed by 730 molecules. The distribution of hydrodynamic diameters of 730NPs in aqueous suspension (Fig. 2b) shows the absence of signals around 10 nm. Therefore, the black dots in Fig. S12 are tentatively assigned to a small quantity of defect or impurity on carbon-coated copper grids, which is commonly observed during TEM studies.

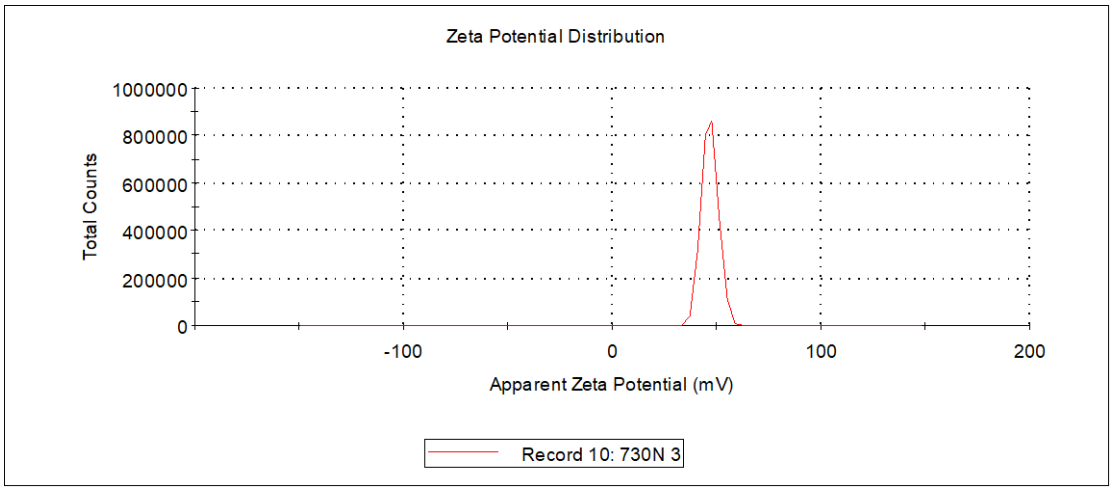

Fig. S13 Zeta-potential distribution of 730 nanoparticles in aqueous medium. The average zeta-potential of 730NPs was measured to be +46.9 mV.

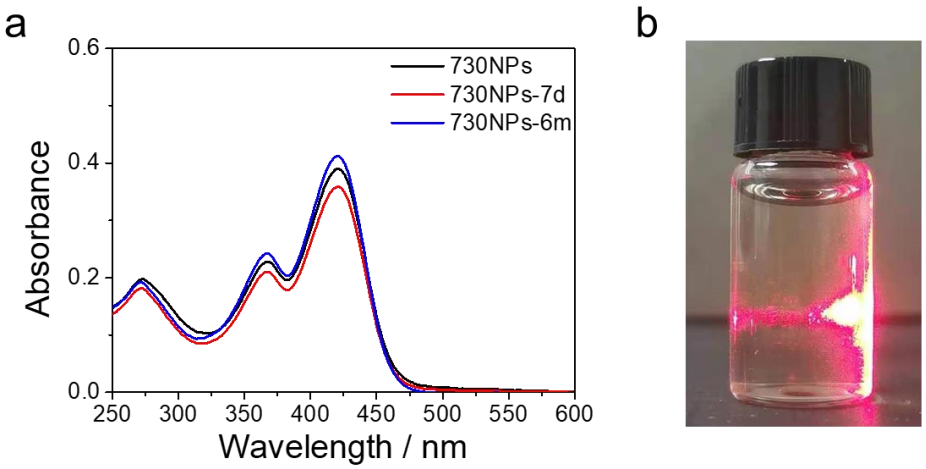

Fig. S14 (a) UV-Vis spectra of fresh-prepared 730NPs and 730NPs after 7-day or 6-month storage. The 730NPs prepared six months ago is still stable as evidenced from their UV-vis spectra and Tyndall effect of the aqueous suspension (b).

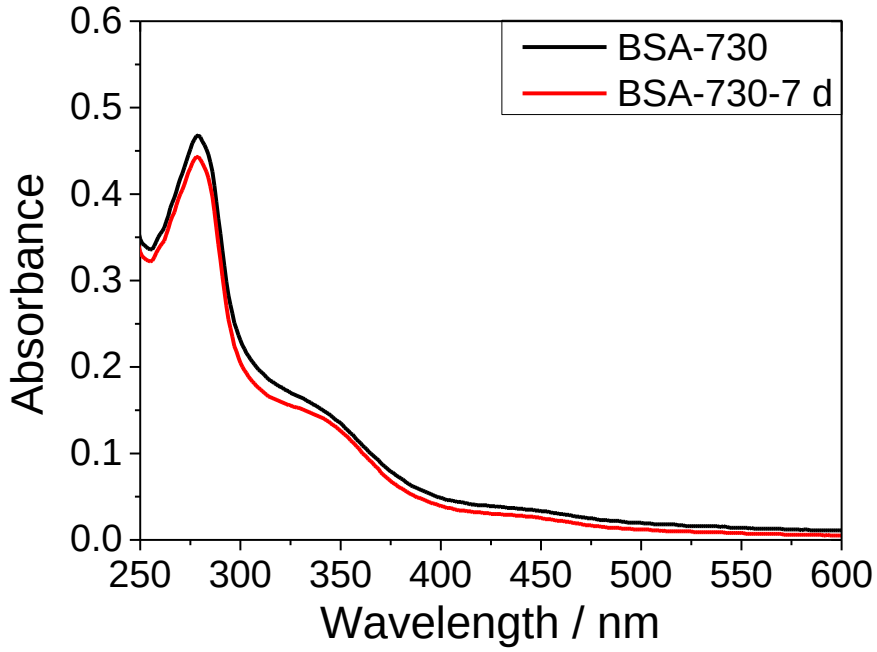

Fig. S15 UV-Vis spectra of fresh-prepared BSA-730 and BSA-730 after 7-day storage.

Table S1. Crystal data and structure refinement for mo_d8v20371_0m.

Identification code	mo_d8v20371_0m	
Empirical formula	C21 H19 F3 O6 S	
Formula weight	456.42	
Temperature	193(2) K	
Wavelength	0.71073 Å	
Crystal system	Triclinic	
Space group	P -1	
Unit cell dimensions	a = 8.291(3) Å	α= 100.873(14)°.
	b = 10.898(5) Å	β= 105.640(13)°.
	c = 11.966(5) Å	γ = 95.465(14)°.
Volume	1010.2(8) $Å^3$	
Z	2	
Density (calculated)	1.500 Mg/m^3	
Absorption coefficient	0.225 mm^{-1}	
F(000)	472.6	
Crystal size	0.150 x 0.120 x 0.070 mm^3	
Theta range for data collection	2.332 to 25.000°.	
Index ranges	-10<=h<=7, -13<=k<=14, -14<=l<=15	

Reflections collected	8367
Independent reflections	3432 [Rint = 0.1021, Rsigma = 0.1739]
Completeness to theta = 25.242°	93.8 %
Absorption correction	Semi-empirical from equivalents
Max. and min. transmission	0.7456 and 0.5661
Refinement method	Full-matrix least-squares on F^2
Data / restraints / parameters	3432 / 65 / 328
Goodness-of-fit on F^2	1.119
Final R indices [I>2sigma(I)]	R1 = 0.0905, wR2 = 0.2011
R indices (all data)	R1 = 0.1823, wR2 = 0.2641
Extinction coefficient	n/a
Largest diff. peak and hole	0.63/-0.69 e.$Å^{-3}$

Table S2. Fractional Atomic coordinates (x 10^4) and equivalent isotropic displacement parameters ($Å^2$x 10^3) for mo_d8v20371_0m. U(eq) is defined as one third of the trace of the orthogonalized U^{ij} tensor.

	x	y	z	U(eq)
S(1)	748(3)	7540(2)	8046(3)	45.9(7)
F(1)	-1296(7)	6209(5)	6045(5)	98(2)
F(2)	1236(8)	5848(7)	6371(7)	111(3)
F(3)	544(11)	7516(7)	5829(6)	128(3)
O(4)	-316(7)	8484(5)	8003(6)	66.2(18)
O(5)	2546(7)	7993(6)	8377(7)	99(2)
O(6)	344(9)	6535(4)	8580(5)	71(2)
C(21)	311(11)	6757(8)	6485(8)	61(2)
S(1A)	250(30)	7320(20)	7980(20)	80
F(1A)	610(50)	5960(30)	6090(40)	80
F(2A)	2150(30)	7760(20)	6640(30)	80
F(3A)	-420(40)	7620(30)	5870(30)	80
O(4A)	-1330(30)	6670(30)	7690(30)	80
O(5A)	540(50)	8680(30)	8420(40)	80
O(6A)	1580(40)	6740(30)	8570(30)	80
C(21A)	690(50)	7180(40)	6550(30)	80
O(1)	-4633(6)	1804(4)	4819(4)	67.0(13)
O(2)	3585(5)	2965(4)	10909(4)	44.4(12)
O(3)	7322(13)	8457(8)	13347(9)	60(3)
O(3A)	6990(50)	8730(30)	13070(30)	78(11)
O(7)	1421(6)	1676(5)	9377(5)	45.4(15)
C(1)	2741(7)	1795(5)	10339(6)	42.6(15)
C(1A)	3585(5)	2965(4)	10909(4)	44.4(12)
C(2)	3372(8)	761(6)	10846(6)	59.6(19)
C(3)	3138(7)	4021(5)	10525(5)	40.0(14)
C(4)	1768(7)	3889(5)	9548(6)	43.3(15)
C(5)	866(7)	2678(5)	8921(6)	42.2(15)
C(6)	1421(6)	1676(5)	9377(5)	45.4(15)
C(7)	-554(7)	2493(5)	7860(5)	40.7(14)
C(8)	-1126(7)	3500(5)	7397(6)	42.9(15)
C(9)	-2470(7)	3313(6)	6373(6)	48.2(16)
C(10)	-3292(7)	2095(6)	5810(6)	47.8(16)

C(11)	-2731(8)	1086(6)	6254(7)	59.7(18)
C(12)	-1399(8)	1261(6)	7259(7)	55.9(18)
C(13)	4185(7)	5200(5)	11233(5)	42.1(15)
C(14)	5581(8)	5210(6)	12191(6)	51.5(16)
C(15)	6584(8)	6313(7)	12869(6)	56.7(18)
C(16)	6210(8)	7454(6)	12576(6)	49.9(16)
C(17)	4859(7)	7485(6)	11622(6)	48.7(16)
C(18)	3856(7)	6353(5)	10946(6)	43.8(15)
C(19)	7025(12)	9633(9)	13085(9)	63(3)
C(19A)	8310(30)	8900(30)	14180(30)	61(9)
C(20)	-5237(9)	2807(7)	4300(7)	75(2)

Table S3. Bond lengths [Å] and angles [°] for mo_d8v20371_0m.

S1-O4	1.417(5)
S1-O5	1.446(6)
S1-O6	1.425(6)
S1-C21	1.823(10)
F1-C21	1.327(9)
F2-C21	1.319(9)
F3-C21	1.278(9)
O1-C10	1.350(7)
O1-C20	1.423(8)
O2-C1	1.352(7)
O2-C3	1.364(6)
C1-C2	1.453(8)
C1-C6	1.333(7)
C1-O7	1.333(7)
C1-C1A	1.352(7)
C3-C4	1.367(8)
C3-C13	1.450(8)
C3-C1A	1.364(6)
C4-C5	1.414(8)
C5-C6	1.374(7)
C5-C7	1.445(8)
C5-O7	1.374(7)
C7-C8	1.387(8)
C7-C12	1.413(8)
C8-C9	1.383(8)
C9-C10	1.387(8)
C10-C11	1.376(8)
C11-C12	1.363(9)
C13-C14	1.390(8)
C13-C18	1.396(7)
C14-C15	1.368(9)
C15-C16	1.395(8)
C16-C17	1.374(8)
C16-O3	1.365(10)
C1	C2
C16-O3A	1.42(3)

C17-C18	1.391(8)
O3-C19	1.404(13)
O3A-C19A	1.44(3)
C21A-S1A	1.83(3)
C21A-F1A	1.32(3)
C21A-F2A	1.28(3)
C21A-F3A	1.25(3)
S1A-O4A	1.35(2)
S1A-O5A	1.46(3)
S1A-O6A	1.41(3)
O5-S1-O4	115.8(4)
O6-S1-O4	116.8(4)
O6-S1-O5	113.3(4)
C21-S1-O4	103.3(4)
C21-S1-O5	101.7(5)
C21-S1-O6	103.2(4)
C20-O1-C10	118.2(5)
C3-O2-C1	122.1(5)
C2-C1-O2	115.9(6)
C6-C1-O2	118.6(5)
C6-C1-C2	125.5(6)
O7-C1-O2	118.6(5)
O7-C1-C2	125.5(6)
O7-C1-C6	0.0
C1A-C1-O2	0.0
C1A-C1-C2	115.9(6)
C1A-C1-C6	118.6(5)
C1A-C1O7	118.6(5)
C4-C3-O2	118.7(5)
C13-C3-O2	115.1(5)
C13-C3-C4	126.2(5)
C1A-C3-O2	0.0
C1A-C3-C4	118.7(5)
C1A-C3C13	115.1(5)
C5-C4-C3	120.7(5)
C6-C5-C4	116.0(6)
C7-C5-C4	122.5(5)
C7-C5-C6	121.5(5)

O7-C5-C4	116.0(6)
O7-C5-C6	0.0
O7-C5-C7	121.5(5)
C5-C6-C1	123.8(5)
C8-C7-C5	121.8(5)
C12-C7-C5	120.3(5)
C12-C7-C8	117.9(6)
C9-C8-C7	121.5(6)
C10-C9-C8	119.4(6)
C9-C10-O1	124.4(6)
C11-C10O1	115.8(6)
C11-C10-C9	119.8(6)
C12-C11-C10	121.2(6)
C11-C12-C7	120.2(6)
C14-C13-C3	120.9(5)
C18-C13-C3	120.9(6)
C18-C13-C14	118.1(6)
C15-C14-C13	121.7(6)
C16-C15-C14	119.0(6)
C17-C16-C15	121.2(6)
O3-C16-C15	111.3(7)
O3-C16-C17	127.5(7)
O3A-C16-C15	133.1(14)
O3A-C16-C17	105.7(13)
O3A-C16-O3	21.8(12)
C18-C17-C16	118.9(6)
C17-C18-C13	121.1(6)
F1-C21-S1	110.0(6)
F2-C21-S1	110.7(6)
F2-C21-F1	106.4(8)
F3-C21-S1	113.3(7)
F3-C21-F1	106.6(8)
F3-C21-F2	109.5(8)
C19-O3-C16	113.9(8)
C5-O7-C1	123.8(5)
C3-C1A-C1	122.1(5)
C19A-O3A-C16	114(2)
F1A-C21A-S1A	107(3)

F2A-C21A-S1A	113(3)
F2A-C21A-F1A	109(3)
F3A-C21A-S1A	109(3)
F3A-C21A-F1A	109(4)
F3A-C21A-F2A	109(3)
O4A-S1A-C21A	104(2)
O5A-S1A-C21A	102(2)
O5A-S1A-O4A	119(3)
O6A-S1A-C21A	99(2)
O6A-S1A-O4A	116(3)
O6A-S1A-O5A	112(3)